Published in final edited form as:

ACS Macro Lett. 2023 June 20; 12(6): 725–732. doi:10.1021/acsmacrolett.3c00144.

Systematic D-amino acid substitutions to control peptide and hydrogel degradation in cellular microenvironments

Kartik Bomb[†], **Qi Zhang**[†], **Eden M. Ford**[†], **Catherine A. Fromen**[†], **April M. Kloxin**[†,&]

[†]Department of Chemical and Biomolecular Engineering, Colburn Laboratory, 150 Academy Street, University of Delaware, Newark, Delaware 19716, United States

[&]Department of Materials Science and Engineering, 201 DuPont Hall, University of Delaware, Newark, Delaware 19716, United States

Abstract

Enzymatically degradable peptides are commonly used as linkers within hydrogels for biological applications; however, controlling the degradation of these engineered peptides with different contexts and cell types can prove challenging. In this work, we systematically examined the substitution of D-amino acids (AAs) for different L-AAs in a peptide sequence commonly utilized in enzymatically-degradable hydrogels (VPMS↓MRGG) to create peptide linkers with a range of different degradation times, in solution and in hydrogels, and investigated the cytocompatibility of these materials. We found that increasing the number of D-AA substitutions increased the resistance to enzymatic degradation both for free peptide and peptide-linked hydrogels; yet, this trend also was accompanied by increased cytotoxicity in cell culture. This work demonstrates the utility of D-AA-modified peptide sequences to create tunable biomaterials platforms tempered by considerations of cytotoxicity, where careful selection and optimization of different peptide designs is needed for specific biological applications.

Graphical Abstract

Author contributions

K.B. and Q.Z. contributed equally to this work.

Supporting Information. Materials and Methods; mass spectrometry figures of synthesized peptides; *in situ* modulus of hydrogels, ^{1}H NMR spectra for PEG-4-Nb and LAP; Representative flow cytometry gating; Tables of statistical analysis for free peptide cytotoxicity and apoptotic population.

The authors declare no competing financial interest.

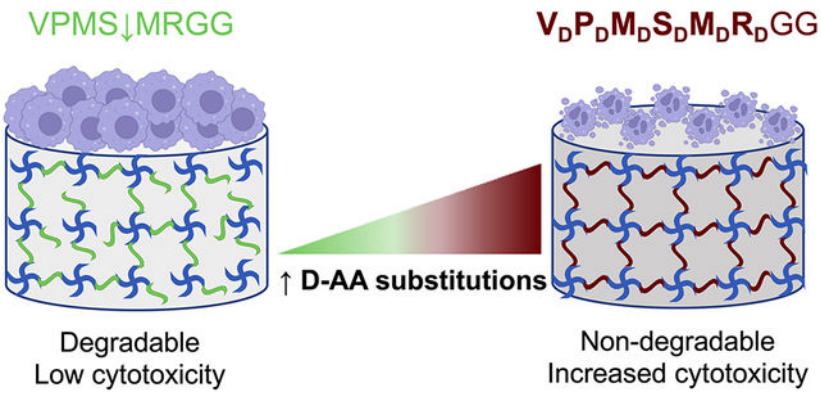

Keywords

Hydrogels; Cell culture; controlled degradation; D-Amino acids; peptides

Synthetic hydrogels have been widely used for different biological applications, including as matrices and scaffolds[1, 2] for cell culture and delivery and as implantable depots[3, 4] for controlled release of therapeutics. Synthetic hydrogels for these applications often are formed with hydrophilic polymers (*e.g.*, poly(ethylene glycol) (PEG), poly(vinyl alcohol) (PVA), modified with vinyl groups) and matrix metalloproteinase (MMP) sensitive linkers (*e.g.*, peptides) to impart responsive degradation in the presence of cell types of interest.[5, 6] These degradable hydrogel platforms have also been shown to promote important cellular functions, including migration[7], proliferation[8], and lineage-specific cell differentiation.[9] Engineered peptide sequences with increased MMP specificity often are used in these systems to facilitate tailored hydrogel degradation profiles by cell-secreted proteolytic enzymes in specific contexts (*e.g.*, *in vitro* two-dimensional or three-dimensional (2D or 3D) cell culture or *in vivo* in the presence of different cell types).[10-13] These peptides are commonly made using L-amino acids (L-AAs) where sequences are inspired by or derived from those found in proteins and allow for controlled peptide degradation in the presence of cell-secreted soluble factors or applied enzymes.[14] While degradation of the peptides and hydrogels is often beneficial, uncontrolled degradation can lead to a significant and premature dissolution of the hydrogel-based synthetic matrix, resulting in deleterious alterations to mechanical properties that influence cellular responses or therapeutic release rates.

Several generalizable strategies have been proposed to control the degradation rate of the peptides, such as modifying the peptide sequence by introducing D-AA[15-18], scrambling the sequence[19], switching amino acids[8], and introducing non-natural amino acids[20] or peptoids[21] in the sequence. Other strategies include modifying the structure of the peptide sequence by alkylation[22], cyclization[23], and glycosylation[24] of the amino acids to impart proteolytic resistance. Amongst these, specific strategies have been utilized to enhance the linker peptide resistance towards enzymatic resistance in hydrogel systems. For example, swapping specific L-AAs with their chiral counterparts (D-AAs) has shown increased resistance to proteolytic degradation, imparting an increased half-life of the linker peptide. This strategy was used to create non-degradable hydrogels with demonstrated utility in

both *in vitro* and *in vivo* applications: the modified peptide sequences contained two D-AA substitutions that were three AA apart and asymmetrically incorporated on either side of the cleavage site to impart stability in the presence of wound healing fibroblasts amongst other cell types.[15] Another strategy to control the MMP-specific peptide degradation is scrambling the peptide sequence (e.g., GPQG↓IAGQ to GPQIGAGQ), which has been utilized to create a non-degradable hydrogel platform.[19] While D-AA substitution has been shown more effective broadly in controlling peptide degradation, some studies with soluble peptides have highlighted an association of D-AAs and D-AA substituted peptides with increased cytotoxicity.[25-27] However, less is known about how systematic substitutions of L-AAs with D-AAs modulates peptide degradation and cellular cytotoxicity in hydrogels.

In this work, we investigated the effect of the systematic substitutions of D-AAs on enzymatic degradation and cytocompatibility of a widely used responsive peptide linker in solution and in hydrogels for achieving a range of degradation times and establishing relevant design rules. Specifically, we first selected the commonly utilized engineered amino acid linker sequence VPMS↓MRGG (VPMS) that is susceptible to cleavage by cell-secreted soluble factors, including MMP2 and MMP9.[10] Next, we created a library of peptides where L-AAs in the linker sequence were substituted with their chiral counterparts and included an additional scrambled peptide version (Figure 1; Supporting Information: Linker peptide sequence design). For benchmarking, we included a previously established D-AA modified VPMS linker sequence (dVPMS1a) that has asymmetric placement of D-AAs relative to the cleavage site as an additional control.[15] Once the peptides were synthesized, we performed enzymatic degradation of both peptides in solution (‘free peptide’) and within hydrogels prepared using different linkers to assess tunable degradation behavior. Finally, we tested the cytotoxicity associated with D-AA-modified peptide linkers using both free peptide and hydrogels to assess the utility of the hydrogel platform for cellular applications. Here, we focused on the culture of macrophage cells (MH-S), innate immune cells that are the ‘first responders’ to changes that occur within various tissue microenvironments and of interest for controlled culture studies of complex immune processes. Taken together, the approaches and insights established here are of utility for the creation of responsive peptide sequences with properties tailored for specific biological applications, including tunable hydrogel platforms with various MMP-sensitive linker sequences.

Peptides were designed with an increasing number of D-AA substitutions adjacent to the cleavage site to evaluate their relative impact on peptide degradation rates and cytocompatibility (Figure 1). All peptides were prepared using microwave-assisted solid-phase peptide synthesis and characterized using mass spectrometry (Figure S1-7). Additionally, the integration of D-AAs in the linker peptides was confirmed by circular dichroism[28 29], where an expected decrease in the negative mean residual ellipticity (MRE) was observed for dVPMS peptides in addition to a random coil confirmation for all the peptides (Figure S12). We first investigated the enzymatic degradation of modified VPMS peptides in response to type IV Collagenase 4 (Cls-4, also known as gelatinase). Cls-4 was selected because the original VPMS sequence has shown increased susceptibility to degradation towards MMP2 (gelatinase A) and MMP9 (gelatinase B), both of which are present in Cls-4 and are known to be important in cellular processes involved in tissue injury and disease including cell migration and proliferation.[10, 14, 30]

Individual peptides in solution (9 mM) were incubated with Cls-4 (10 μg/mL) for 24 hours and the enzymatic degradation of each peptide was determined both qualitatively and quantitatively. Mass spectrometry then was used to determine the relative fraction of intact, undegraded peptide over time to assess the degree to which D-AA substitutions in the peptide sequence or scrambling of the L-AAs within the peptide sequence increased the resistance to enzymatic degradation. For all the designed peptides, the peak associated with the intact, undegraded sequence was measured at the 0-hour time point and was between 1.75 – 1.9 minutes as highlighted in the ultra performance liquid chromatography-tandem mass spectrometry (UPLC-MS) chromatograms, whereas cleaved peptide products from later time points were observed further downfield (Figure 1).

We had hypothesized that, in the presence of Cls-4, an increasing number of D-AA substitutions or scrambling of the VPMS peptide sequence would show a relatively slower rate of degradation and a higher fraction of undegraded peptide peak compared to the original VPMS sequence, which completely degraded in 24 hours (Figure 1A). Interestingly, both dVPMS1 and dVPMS1a, which consisted of 1 D-AA substitution on each side of the cleavage site (2 D-AA substitutions per peptide sequence symmetrically or asymmetrically), showed partial degradation with the presence of the undegraded peptide peak between 1.75 – 1.9 minutes in addition to degraded peptide fragments between 1.99 – 2.25 minutes (Figure 1B and 1E). Importantly, as we increased the number of D-AAs in the peptide sequence to 2 (dVPMS2, 4 total substitutions) or 3 D-AA substitutions on each side of cleavage site (dVPMS3, 6 total substitutions), we observed that both dVPMS2 (Figure 1C) and dVPMS3 (Figure 1D) were resistant to enzymatic degradation under the experimental conditions probed, as the undegraded peptide peak was completely intact without the presence of additional peaks of degraded peptide fragments over 24 hours. Surprisingly, scrambling of the L-AAs within the VPMS sequence (sVPMS) did not impart resistance to enzymatic degradation. While increased resistance to proteolytic degradation has previously been reported with scrambling of other enzymatically degradable peptide sequences (*e.g.*, GPQIGAGQ)[19], employing the same strategy for VPMS peptide failed to make the sequence non-degradable. Overall, these observations supported the hypothesis that increased D-AA substitutions resulted in increased resistance to enzymatic degradation, thereby increasing the half-life of the peptide, and highlights the importance of careful selection and evaluation of scrambled sequences aimed at controlling peptide degradation.

Next, we quantified the kinetic parameter (k_{cat}) for all the degradable peptides by fluorometric assay[31] and fitting of Michaelis-Menten kinetics to quantify the rate of peptide degradation (Figure 1G). Specifically, peptides were incubated with Cls-4 solution and, at specific time points, aliquots were incubated with fluorescamine solution to quantify changes in fluorescence intensity and determine degradation kinetics.[32] Based on the mass spectrometry analysis, we had identified 3 groups of peptides depending on their degradation characteristics under the conditions probed: *i)* 'completely degradable' (VPMS and sVPMS), *ii)* 'quickly degrading' (dVPMS1 and dVPMS1a), and *iii)* 'slowly degrading' (dVPMS2 and dVPMS3) peptides and measured k_{cat} values follow these groupings.

For the completely degradable peptide group, the k_{cat} value for the original VPMS sequence was ~5.80 s^{-1}, which is in accordance with the k_{cat} values reported in the literature. sVPMS

had a slightly higher k_{cat} value (~6.34 s^{-1}) that was statistically similar to the VPMS sequence. This trend, although not statistically significant, is consistent with UPLC-MS observations, where at 6-hour time point a higher fraction of the undegraded peptide peak was observed for VPMS compared to sVPMS (Figure 1A and 1F). For the quickly degrading peptide group, k_{cat} values of both dVPMS1 (~1.44 s^{-1}) and dVPMS1a (~0.59 s^{-1}) were significantly lower compared to VPMS, consistent with the UPLC-MS results showing slower peptide degradation upon D-AA substitutions. While k_{cat} for both dVPMS1 and dVPMS1a were statistically similar, dVPMS1a showed a lower k_{cat} value compared to dVPMS1, where similar trends were observed with UPLC-MS analysis with a relatively higher fraction of undegraded peptide in dVPMS1a (Figure 1E) compared to dVPMS1 at 24 h (Figure 1B). As expected based on UPLC-MS analysis, no degradation was detected for dVPMS2 and dVPMS3 (k_{cat} ~ 0).

We next sought to investigate the degradation of the hydrogels prepared using the different peptide designs. Hydrogels were formed by a photoinitiated thiol-ene reaction between dithiol linker peptides (9 mM thiol), monothiol pendant peptide (2 mM thiol), and norbornenes presented by functionalized 4-arm PEG (11 mM norbornene; M_n ~ 10 kDa) at 1:1 stoichiometric ratio between thiol and norbornene (365 nm at 10 mW/cm^2 for 5 min), where the pendant peptide was integrated to allow cell attachment in subsequent studies. *In situ* rheometry was performed to confirm the elastic moduli of the hydrogels prepared using different peptide linkers were similar to each other (Figure S8) and representative of soft, loose connective tissues (between 2-3 kPa).[33, 34] To measure hydrogel degradation, equilibrium swollen hydrogels were incubated in Cls-4 (10 μg/mL) solution, and the change in dry hydrogel weight over 24 hours was quantified.

We hypothesized, similar to the free peptide degradation, that we would observe 3 groups of hydrogels under the conditions probed: completely degradable (VPMS and sVPMS), quickly degrading (dVPMS1 and dVPMS1a), and slowly degrading (dVPMS2 and dVPMS3) hydrogels. As expected, hydrogels prepared using VPMS and sVPMS completely degraded within 24 hours and showed a similar degradation profile at each time point, whereas hydrogels prepared using dVPMS2 and dVPMS3 were completely resistant to enzymatic degradation at each time point measured within 24 hours (Figure 2). For the quickly degrading hydrogels prepared with dVPMS1 and dVPMS1a linkers, ~50% reduction in the hydrogel dry weight was observed along with reduced structural integrity, as highlighted in the representative images (Figure 2). Similar to the trends observed with free peptide degradation, dVPMS1a hydrogels initially showed increased degradation resistance compared to dVPMS1 hydrogels; however, by 24 hours, both the hydrogels (dVPMS1 and 1a) showed similar degradation profiles. Finally, we also performed hydrogel degradation studies for select conditions (VPMS, sVPMS, and dVPMS3) in the presence of cell-secreted soluble factors by incubating the hydrogels in the conditioned media obtained from MH-S cells (Figure S14). Similar to collagenase degradation, both VPMS and sVPMS-linked hydrogels completely degraded within 48 hours, whereas no degradation was observed in the dVPMS3-linked hydrogel, indicating cell-secreted proteases can cause significant cleavage of sequences that can be tuned by D-AA substitution.

Interestingly, dVPMS1a[15] linked hydrogels have been shown to be non-degradable in the presence of collagenase (0.2 – 20 U/mL; type not noted) for 8h at 37 °C, whereas in our hands, Cls-4 resulted in partial hydrogel degradation over similar time frames. We hypothesize that this difference in degradability is due to differences in the enzymes used for peptide degradation: in particular, VPMS exhibits an increased rate of degradation in the presence of MMP2 and MMP9 relative to other MMPs, both of which are present in Cls-4, and may explain why only partial resistance to enzymatic degradation for dVPMS1a was observed in the current study. Overall, our results demonstrate that proteolytic degradation of both free peptide and peptide-linked hydrogels can be effectively tuned by substituting D-AAs in the peptide sequence.

Finally, we investigated the utility of modified peptides in cell culture. Specifically, we examined the cytotoxicity of free peptides and peptide-linked hydrogels with a commonly used MH-S macrophage cell line, as macrophages can quickly respond to the changes in their surrounding microenvironment. To determine cytotoxicity, we measured the metabolic activity of cells using an alamarBlue assay, qualitatively examined cell morphology, and then quantified necrosis and apoptosis with flow cytometry.

For probing cellular responses, we first assessed the differences in the metabolic activity of the cells after incubating the cells with free peptides over a range of concentrations for 24 hours and normalizing the metabolic activity to cells without any peptides (Figure 3A). At low peptide concentrations (0.001 mM and 0.01 mM), we did not observe any statistical differences in the metabolic activity of cells when incubated with the different peptides (Table S1). However, as the concentration of the peptides increased to 0.1 mM and 1 mM, cells incubated with D-AA-modified peptides showed statistically lower metabolic activity (Table S1). At 0.1 mM, metabolic activity of MH-S cells with dVPMS2 and dVMPS1a were statistically lower compared to VPMS. At 1 mM, cells incubated with any of the D-AA peptides showed statistically lower metabolic activity compared to VPMS. At the highest peptide concentration (5 mM), all the peptides resulted in lower metabolic activity of MH-S cells; however, VPMS and sVPMS still showed the highest metabolic activity, whereas dVPMS2 and dVMPS1a showed statistically lower metabolic activity compared to VPMS (Table S1). For all the peptide concentrations, cells incubated with sVPMS showed similar metabolic activity compared to the VPMS sequence, both of which have strictly L-AAs. Qualitative examination of cell morphology further supported these observations: while a regular cell morphology was observed in the presence of both VPMS and sVPMS peptides, an irregular cell morphology with increased cell shrinkage was observed with the D-AA substitute sequences (Figure 3B), indicative of cell stress and potentially suggesting that the presence of D-AAs may induce apoptosis. Overall, the introduction of D-AAs at higher peptide concentrations lowered the metabolic activity of the cells and resulted in an irregular morphology; however, no discernable trends in the metabolic activity or morphology were observed with respect to the number of D-AAs present in the sequence.

We next examined the cytotoxicity of peptide-linked hydrogels. Based on our previous work,[35] all of the hydrogels incorporated 2 mM of integrin binding peptide ($CGGPHSRNG_{10}RGDSP$) to promote cell attachment to the hydrogel-based synthetic matrix, and samples were washed and allowed to equilibrium swell for 24 hours before

cell seeding. Cells were seeded on the hydrogels for 24 hours to allow attachment and response, after which cytotoxicity assessments were performed. First, we measured the metabolic activity: cells seeded on any of the dVPMS peptide linked hydrogels showed statistically lower metabolic activity compared to VPMS hydrogels, whereas responses on sVPMS hydrogels were statistically the same as those on VPMS hydrogels (Figure 4A). Again, no discernable trend in metabolic activity was observed with respect to the number of D-AAs present in the sequence.

To further understand the potential origin of the observations decreased metabolic activity, the apoptotic profiles of cells were examined with flow cytometry, analyzing the percentage of cells stained with Zombie Yellow (ZY) and Apotracker green (Apo). ZY stains dead cells, whereas Apo stains membrane translocated phosphatidylserine present on apoptotic cells that will subsequently undergo programmed cell death. By applying an appropriate gating strategy, we were able to identify and quantify different cell populations for each peptide condition: the percentage of (i) Live Cells (ZY−/Apo−), (ii) Early apoptotic cells (ZY−/Apo+), (iii) Late Apoptotic Cells (ZY+/Apo+), and (iv) Necrotic Cells (ZY+/Apo−) (Figure 4B).

Cells seeded on VPMS and sVPMS linked hydrogel had greater than 90% live cell population, a typical viability for cells observed after passaging and seeding. However, for all dVPMS linker hydrogels, a statistically significant shift in the population of cells from Live to Late Apoptotic was observed (Figure 4C, Table S2). Interestingly, as the number of D-AAs in the peptide sequence increased from 2 D-AAs (dVPMS1) to 6 D-AAs (dVPMS3), a statistically higher fraction of Late Apoptotic cells and a statistically lower fraction of live cells were observed (Figure 4C, Table S2). We speculate that the presence of D-AAs in the peptide linkers results in increased oxidative damage to the cells, as highlighted by increased apoptotic cell population along with shrinking and stressed cell morphology when incubated with D-AA peptides. For example, Bardaweel *et al.*[27] have shown similar cytotoxicity results associated with D-AAs in soluble peptides and demonstrated that D-AA oxidation by cells using D-amino-acid oxidase results in the generation of hydrogen peroxide, causing oxidative damage and lower cell viability. Overall, our results demonstrate that increasing the number of D-AAs in the peptide sequence is associated with higher apoptosis of MH-S cells.

In summary, we have shown how D-AAs can be effectively used in responsive peptides for tunable degradation over different timescales in solution and hydrogels for cellular applications, where increasing the D-AAs in the peptide sequence imparts increasing resistance to enzymatic degradation and can even be used to produce stable peptide linkers with similar chemical identities. However, the introduction of D-AAs also is associated with increased cytotoxicity for macrophages, which may be cell-type specific. In this context, these findings have the potential to enable peptide designs not only with precisely tuned degradation for applications of interest, but also for suppressing or promoting immune cell responses amongst other cellular responses of interest. Furthermore, we report that scrambling the VPMS peptide sequence was not effective in reducing the peptide degradation, highlighting the need for careful selection and optimization of the scrambled sequence for achieving controlled peptide degradation or stability. In general, the strategies

highlighted here could be easily employed to design and evaluate other enzymatically responsive peptides with tunable degradability by integrating increasing numbers of D-AA substitutions into other known degradable peptide sequences. Such tunable hydrogels offer considerable opportunities for various *in vitro* and *in vivo* applications such as creation of 2D or 3D hydrogel culture platforms for understanding complex cell interactions in diseased states or for *in vivo* applications as drug delivery vehicles for different therapeutics with a localized and targeted release profile.

Supplementary Material

Refer to Web version on PubMed Central for supplementary material.

Acknowledgments

This work was supported by Collins fellowship (Bomb), University of Delaware Undergraduate Research Program (Qi), NIH Director's New Innovator Award (DP2HL152424, Kloxin), and NIH NIGMS MIRA Award (R35GM142866A, Fromen). The authors thank Dr. Lina Pradhan for her suggestions on peptide cytotoxicity studies and Samantha Cassel for her valuable insights and feedback on quantifying peptide degradation. Additionally, the authors acknowledge the use of facilities and instrumentation supported by the National Science Foundation through the University of Delaware Materials Research Science and Engineering Center (DMR-2011824) and the National Institute of General Medical Sciences, part of the National Institutes of Health, through the Delaware COBRE (P20GM104316). Table of Content figure was prepared using BioRender.com.

References

(1). Rosales AM; Anseth KS The design of reversible hydrogels to capture extracellular matrix dynamics. Nature Reviews Materials 2016, 1 (2), 1–15.

(2). Rizwan M; Baker AE; Shoichet MS Designing hydrogels for 3D cell culture using dynamic covalent crosslinking. Advanced Healthcare Materials 2021, 10 (12), 2100234.

(3). Leach DG; Young S; Hartgerink JD Advances in immunotherapy delivery from implantable and injectable biomaterials. Acta biomaterialia 2019, 88, 15–31. [PubMed: 30771535]

(4). Niazi M; Alizadeh E; Zarebkohan A; Seidi K; Ayoubi-Joshaghani MH; Azizi M; Dadashi H; Mahmudi H; Javaheri T; Jaymand M Advanced bioresponsive multitasking hydrogels in the new era of biomedicine. Advanced Functional Materials 2021, 31 (41), 2104123.

(5). Chen W; Zhou Z; Chen D; Li Y; Zhang Q; Su J Bone regeneration using MMP-cleavable peptides-based hydrogels. Gels 2021, 7 (4), 199. [PubMed: 34842679]

(6). Wiley KL; Sutherland BP; Ogunnaike BA; Kloxin AM Rational Design of Hydrogel Networks with Dynamic Mechanical Properties to Mimic Matrix Remodeling. Advanced Healthcare Materials 2022, 11 (7), 2101947.

(7). Jung M; Skhinas JN; Du EY; Tolentino MK; Utama RH; Engel M; Volkerling A; Sexton A; O'Mahony AP; Ribeiro JC A high-throughput 3D bioprinted cancer cell migration and invasion model with versatile and broad biological applicability. Biomaterials Science 2022, 10 (20), 5876–5887. [PubMed: 36149407]

(8). Bott K; Upton Z; Schrobback K; Ehrbar M; Hubbell JA; Lutolf MP; Rizzi SC The effect of matrix characteristics on fibroblast proliferation in 3D gels. Biomaterials 2010, 31 (32), 8454–8464. [PubMed: 20684983]

(9). Ren Y; Zhang H; Qin W; Du B; Liu L; Yang J A collagen mimetic peptide-modified hyaluronic acid hydrogel system with enzymatically mediated degradation for mesenchymal stem cell differentiation. Materials Science and Engineering: C 2020, 108, 110276. [PubMed: 31923951]

(10). Turk BE; Huang LL; Piro ET; Cantley LC Determination of protease cleavage site motifs using mixture-based oriented peptide libraries. Nature biotechnology 2001, 19 (7), 661–667.

(11). Smithmyer ME; Spohn JB; Kloxin AM Probing fibroblast activation in response to extracellular cues with whole protein-or peptide-functionalized step-growth hydrogels. ACS biomaterials science & engineering 2018, 4 (9), 3304–3316. [PubMed: 32494587]

(12). Rehmann MS; Luna JI; Maverakis E; Kloxin AM Tuning microenvironment modulus and biochemical composition promotes human mesenchymal stem cell tenogenic differentiation. Journal of Biomedical Materials Research Part A 2016, 104 (5), 1162–1174. [PubMed: 26748903]

(13). Patterson J; Hubbell JA Enhanced proteolytic degradation of molecularly engineered PEG hydrogels in response to MMP-1 and MMP-2. Biomaterials 2010, 31 (30), 7836–7845. [PubMed: 20667588]

(14). Nagase H; Fields GB Human matrix metalloproteinase specificity studies using collagen sequence-based synthetic peptides. Peptide Science 1996, 40 (4), 399–416. [PubMed: 8765610]

(15). Lueckgen A; Garske DS; Ellinghaus A; Mooney DJ; Duda GN; Cipitria A Enzymatically-degradable alginate hydrogels promote cell spreading and in vivo tissue infiltration. Biomaterials 2019, 217, 119294. [PubMed: 31276949]

(16). Tugyi R; Uray K; Iván D; Fellinger E; Perkins A; Hudecz F Partial D-amino acid substitution: Improved enzymatic stability and preserved Ab recognition of a MUC2 epitope peptide. Proceedings of the National Academy of Sciences 2005, 102 (2), 413–418.

(17). Griffin DR; Archang MM; Kuan C-H; Weaver WM; Weinstein JS; Feng AC; Ruccia A; Sideris E; Ragkousis V; Koh J Activating an adaptive immune response from a hydrogel scaffold imparts regenerative wound healing. Nature materials 2021, 20 (4), 560–569. [PubMed: 33168979]

(18). Restu WK; Yamamoto S; Nishida Y; Ienaga H; Aoi T; Maruyama T Hydrogel formation by short D-peptide for cell-culture scaffolds. Materials Science and Engineering: C 2020, 111, 110746. [PubMed: 32279773]

(19). Lin L; Marchant RE; Zhu J; Kottke-Marchant K Extracellular matrix-mimetic poly (ethylene glycol) hydrogels engineered to regulate smooth muscle cell proliferation in 3-D. Acta biomaterialia 2014, 10 (12), 5106–5115. [PubMed: 25173839]

(20). Lu J; Xu H; Xia J; Ma J; Xu J; Li Y; Feng J D-and unnatural amino acid substituted antimicrobial peptides with improved proteolytic resistance and their proteolytic degradation characteristics. Frontiers in Microbiology 2020, 11, 563030. [PubMed: 33281761]

(21). Austin MJ; Schunk H; Watkins C; Ling N; Chauvin J; Morton L; Rosales AM Fluorescent peptomer substrates for differential degradation by metalloproteases. Biomacromolecules 2022, 23 (11), 4909–4923. [PubMed: 36269900]

(22). Kaminker R; Anastasaki A; Gutekunst WR; Luo Y; Lee S-H; Hawker CJ Tuning of protease resistance in oligopeptides through N-alkylation. Chemical Communications 2018, 54 (69), 9631–9634. [PubMed: 30095837]

(23). Wolfe JM; Fadzen CM; Holden RL; Yao M; Hanson GJ; Pentelute BL Perfluoroaryl bicyclic cell-penetrating peptides for delivery of antisense oligonucleotides. Angewandte Chemie 2018, 130 (17), 4846–4849.

(24). Tortorella A; Leone L; Lombardi A; Pizzo E; Bosso A; Winter R; Petraccone L; Del Vecchio P; Oliva R The impact of N-glycosylation on the properties of the antimicrobial peptide LL-III. Scientific Reports 2023, 13 (1), 3733. [PubMed: 36878924]

(25). Zhang Z; Li B; Cai Q; Qiao S; Wang D; Wang H; Zhang H; Yang Y; Meng W Synergistic effects of D-arginine, D-methionine and D-histidine against Porphyromonas gingivalis biofilms. Biofouling 2021, 37 (2), 222–234. [PubMed: 33682548]

(26). Birch D; Christensen MV; Staerk D; Franzyk H; Nielsen HM Stereochemistry as a determining factor for the effect of a cell-penetrating peptide on cellular viability and epithelial integrity. Biochemical Journal 2018, 475 (10), 1773–1788. [PubMed: 29686042]

(27). Bardaweel SK; Abu-Dahab R; Almomani NF An in vitro based investigation into the cytotoxic effects of D-amino acids. Acta Pharmaceutica 2013, 63 (4), 467–478. [PubMed: 24451072]

(28). Hilderbrand AM; Ford EM; Guo C; Sloppy JD; Kloxin AM Hierarchically structured hydrogels utilizing multifunctional assembling peptides for 3D cell culture. Biomaterials science 2020, 8 (5), 1256–1269. [PubMed: 31854388]

(29). Greenfield NJ; Fasman GD Computed circular dichroism spectra for the evaluation of protein conformation. Biochemistry 1969, 8 (10), 4108–4116. [PubMed: 5346390]

(30). Kuczek DE; Larsen AMH; Thorseth M-L; Carretta M; Kalvisa A; Siersbæk MS; Simões AMC; Roslind A; Engelholm LH; Noessner E Collagen density regulates the activity of tumor-infiltrating T cells. Journal for immunotherapy of cancer 2019, 7 (1), 1–15. [PubMed: 30612589]

(31). Udenfriend S; Stein S; Boehlen P; Dairman W; Leimgruber W; Weigele M Fluorescamine: a reagent for assay of amino acids, peptides, proteins, and primary amines in the picomole range. Science 1972, 178 (4063), 871–872. [PubMed: 5085985]

(32). Lutolf MP; Lauer-Fields JL; Schmoekel HG; Metters AT; Weber FE; Fields GB; Hubbell JA Synthetic matrix metalloproteinase-sensitive hydrogels for the conduction of tissue regeneration: engineering cell-invasion characteristics. Proceedings of the National Academy of Sciences 2003, 100 (9), 5413–5418.

(33). Iivarinen JT; Korhonen RK; Jurvelin JS Experimental and numerical analysis of soft tissue stiffness measurement using manual indentation device–significance of indentation geometry and soft tissue thickness. Skin Research and Technology 2014, 20 (3), 347–354. [PubMed: 24267492]

(34). Sicard D; Haak AJ; Choi KM; Craig AR; Fredenburgh LE; Tschumperlin DJ Aging and anatomical variations in lung tissue stiffness. American Journal of Physiology-Lung Cellular and Molecular Physiology 2018, 314 (6), L946–L955. [PubMed: 29469613]

(35). Bomb K; Pradhan L; Zhang Q; Jarai BM; Bhattacharjee A; Burris DL; Kloxin AM; Fromen CA Destructive fibrotic teamwork: how both microenvironment stiffness and profibrotic interleukin 13 impair alveolar macrophage phenotype and function. Biomaterials Science 2022, 10 (19), 5689–5706. [PubMed: 36018297]

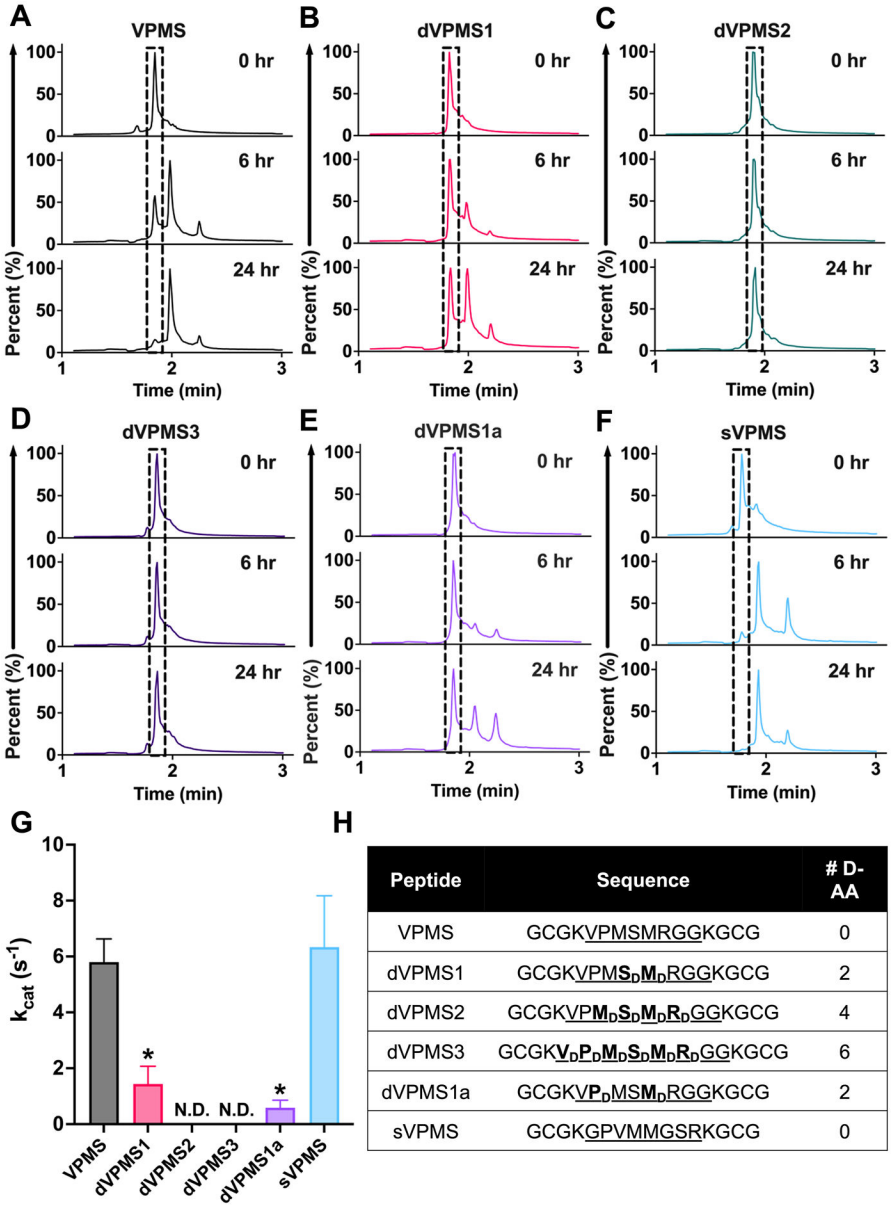

Peptide	Sequence	# D-AA
VPMS	GCGKVPMSMRGGKGCG	0
dVPMS1	GCGKVPM**S$_D$M$_D$**RGGKGCG	2
dVPMS2	GCGKVP**M$_D$S$_D$M$_D$R$_D$**GGKGCG	4
dVPMS3	GCGK**V$_D$P$_D$M$_D$S$_D$M$_D$R$_D$**GGKGCG	6
dVPMS1a	GCGKV**P$_D$**MS**M$_D$**RGGKGCG	2
sVPMS	GCGKGPVMMGSRKGCG	0

Figure 1. Degradation behavior of different peptide designs in solution.

Peptides were incubated with Cls-4, and peptide degradation was determined qualitatively using UPLC-MS and quantitatively using fluorometric assay to determine k_{cat} based on Michaelis-Menten kinetics. (A-F) UPLC-MS chromatograms of different peptide designs (9 mM) over time upon incubation with Cls-4 (10 μg/mL) over time. Dashed box highlights the non-degraded peptide peak. (G) Measured k_{cat} based on Michaelis-Menten kinetics using fluorometric assay ($n \geq 3$). (H) List of peptide designs used in this study. (*) signifies $p < 0.05$. Statistical significance for k_{cat} values was determined using one-way ANOVA with Tukey's test.

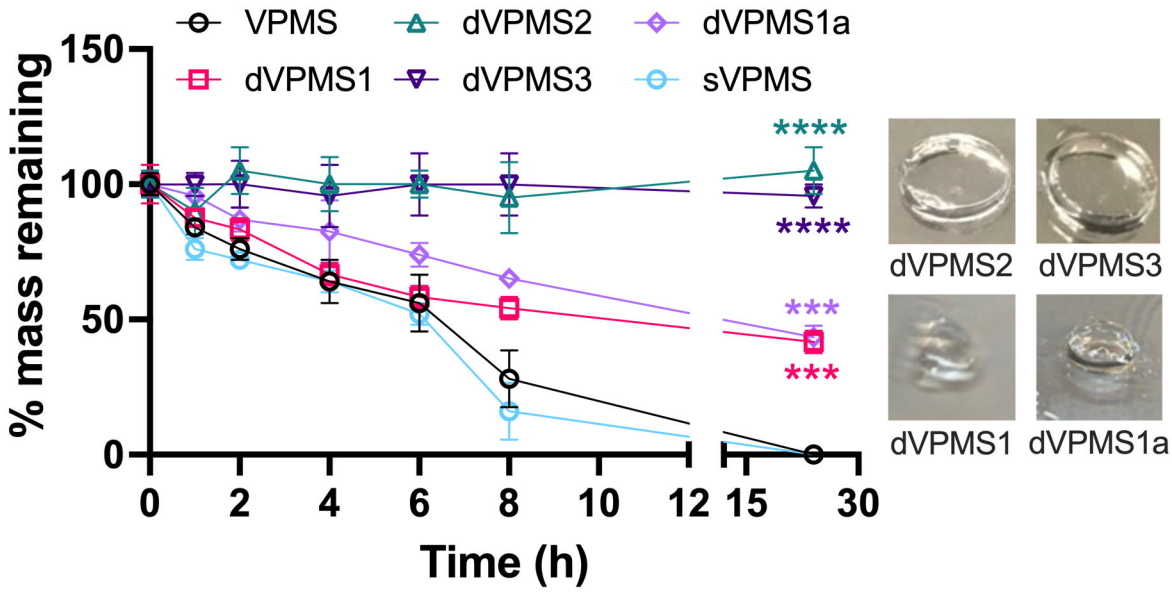

Figure 2. Degradation behavior of different peptide-linked hydrogels.

Hydrogels (n=3) were incubated with Cls-4 (10 μg/mL), and their mass loss was monitored to assess their degradation over time. Statistical significance for mass remaining (%) at 24-hour time point relative to VPMS linker hydrogels was determined using two-way ANOVA with Tukey's test. Representative images of hydrogels at 24-hour timepoint.

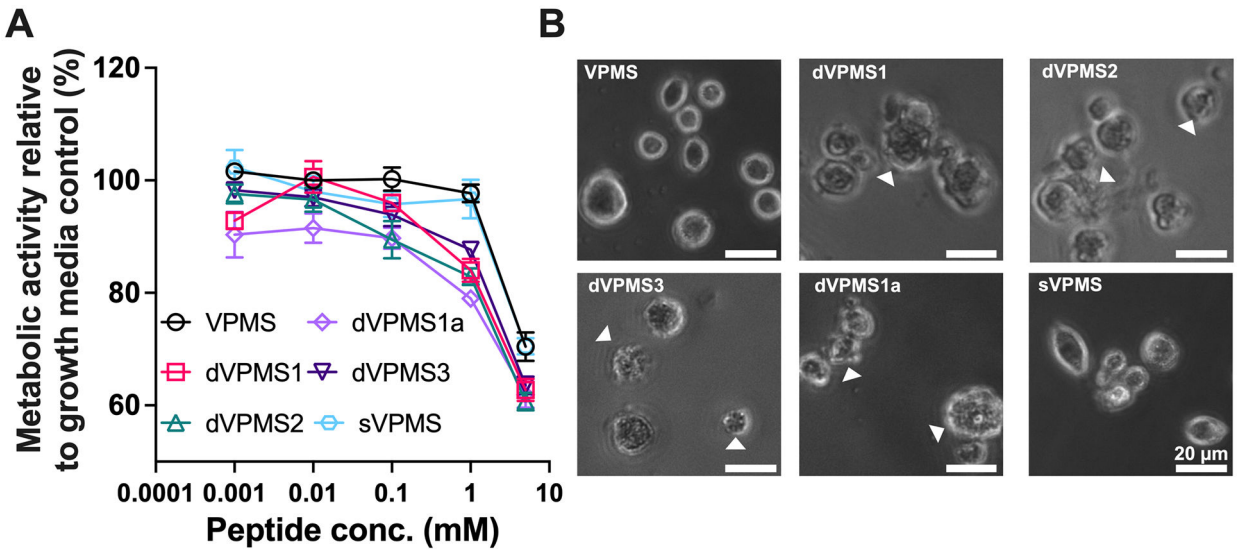

Figure 3. Examination of cytotoxicity associated with different peptide designs.

Free peptides were incubated with macrophages (MH-S cells), and cell metabolic activity (alamarBlue assay) and morphology (brightfield microscopy) were examined for any indication of cytotoxicity. (A) Free peptides, at different concentrations, were incubated with MH-S cells for 24 hours, and changes in metabolic activity relative to cells without any peptide (growth media control) were quantified ($n \geq 3$). Statistical significance for relative changes in metabolic activity at 24-hour time point was determined using two-way ANOVA (Table S1). (B) Representative images of MH-S cells incubated with free peptide. Peptides with D-AA substitution resulted qualitatively in an irregular cell morphology, with increased granularity and diffuse, non-uniform cell walls, indicative of stress (indicated by white arrows).

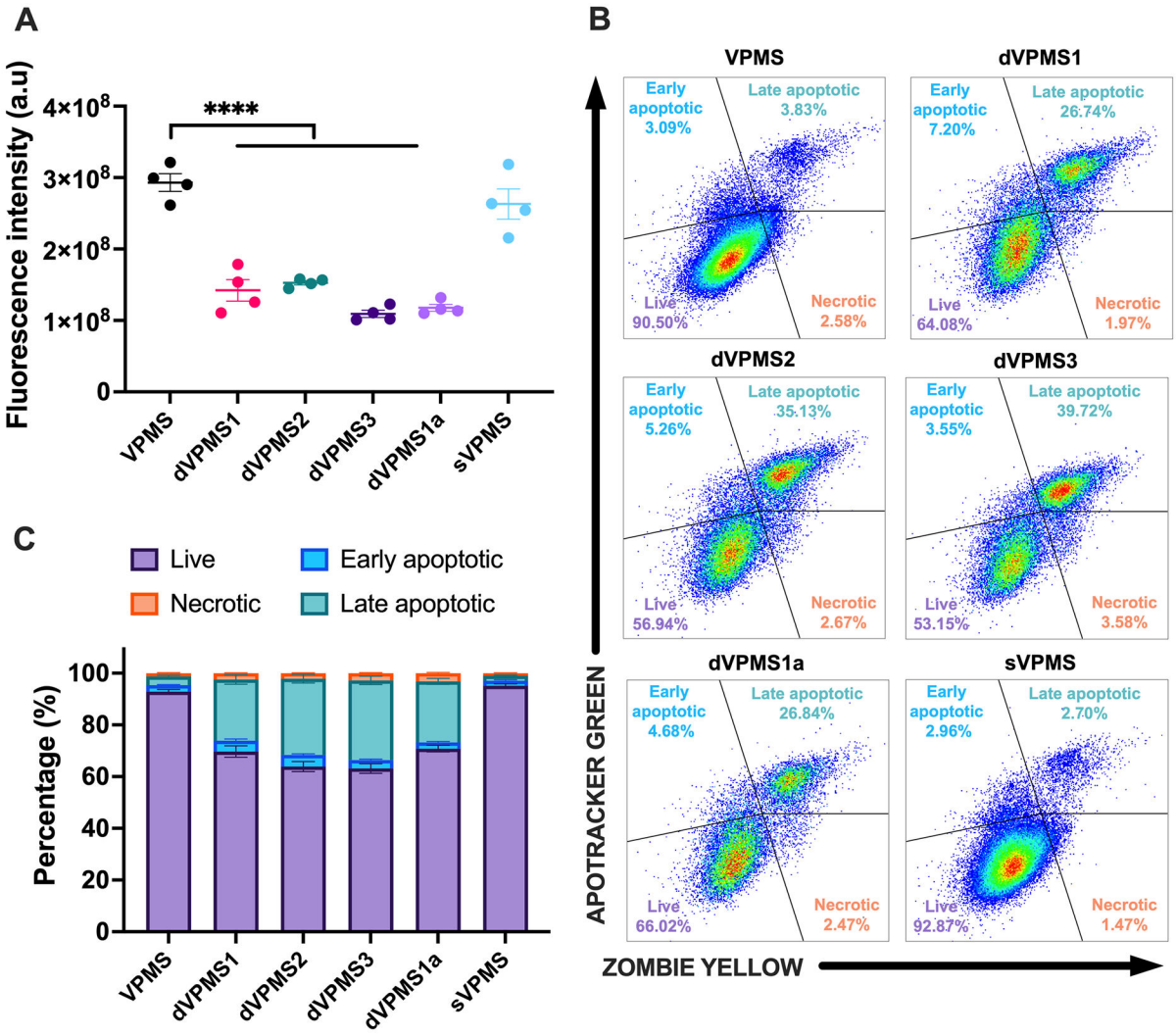

Figure 4. Examination of cytotoxicity of different peptide linked hydrogels.

MH-S cells were seeded on hydrogels prepared with different peptide linkers, and cell health was assessed by metabolic activity measurements and quantification of the apoptotic profiles of cells using flow cytometry. (A) Metabolic activity of cells seeded on hydrogels was measured using the alamarBlue assay, where fluorescence of the metabolized dye in culture media was measured on a plate reader (Excitation: 560, Emission: 590) ($n = 4$). All conditions were compared to cells on the VPMS-linked hydrogels. (****) signifies $p < 0.0001$. Statistical significance for metabolic activity was determined using one-way ANOVA with Tukey's test. (B) Representative flow cytometry gating to identify apoptotic cell populations. Zombie Yellow (ZY) stains dead cells, and Apotracker Green (Apo) stains membrane translocated phosphatidylserine present on apoptotic cells: (i) Live Cells (ZY−/Apo−), (ii) Early apoptotic cells (ZY−/Apo+), (iii) Late Apoptotic Cells (ZY+/Apo+), and (iv) Necrotic Cells (ZY+/Apo−). (C) Quantification of different cell populations obtained from each hydrogel condition ($n \geq 3$). Statistical differences between peptides for different cell populations was determined using two-way ANOVA with Tukey's test.